International Journal of Physics, 2022, Vol. 10, No. 2, 102-110
Available online at http://pubs.sciepub.com/ijp/10/2/3
Published by Science and Education Publishing
DOI:10.12691/ijp-10-2-3

The Substantive Characteristics of Layered PbX (X=S, Se, and Te) Compounds: An ab-inito Investigations

Humaira Takia[1,*], Md. Afjalur Rahman[2], Rahman Moshiur[3], M.M. Rahaman[4], Khokon Hossen[1]

[1]Department of Physics and Mechanical Engineering, Patuakhali Science and Technology University, Dumki, Patuakhali-8602, Bangladesh
[2]Department of Physics, Pabna University of Science and Technology, Pabna-6600, Bangladesh
[3]Department of Physics, Jahangirnagar University, Savar, Dhaka-1342, Bangladesh
[4]Department of Mathematics, Patuakhali Science and Technology University, Dumki, Patuakhali-8602, Bangladesh
*Corresponding author: humairapme@pstu.ac.bd

Received March 02, 2022; Revised April 03, 2022; Accepted April 08, 2022

Abstract In the impending lesson, we explore the substantive features of PbX (S, Se and Te) such as structural, elastic, electronic and optical properties using first principle calculations based on the density functional theory. Generalized gradient approximation (GGA-PBEsol) is used as an exchange-correlation functional for the structural properties of the different crystal phases. For all phases, the optimized lattice parameters display a strong covenant with the available experimental data. The three independent elastic constants (C_{11}, C_{12}, and C_{44}) for all three compounds are positive and fulfill the Born stability criteria, which ensures that all phases possess the mechanical stability in nature. The most significant elastic properties like Bulk modulus (B), shear modulus (G), Young's modulus (Y), Poisson's ratio (v) and elastic anisotropy (A) of the cubic-type structure of PbX (X=S, Se and Te) are estimated and observed under ambient pressure. The Cauchy pressure and Pugh's ratio reveals that all compounds exhibit brittle nature and the band structure analysis ensures the semi-metallic character with a narrow band gap of all these phases. The obtained values of band gap are 0.23 for PbS, 0.15 eV for PbSe, and 0.58 eV for PbTe respectively. At last, it has been obtained and smeared the several optical properties such as absorption, conductivity, reflectivity, loss function, dielectric function and refractive index at the polarization vector [100] of PbX (X=S,Se and Te) in details. The higher reflectivity spectra of these compounds in the Infrared and ultraviolet regions demonstrate promise as excellent shielding materials for avoiding solar heating.

Keywords: *Pb-based compounds, first principle study, density functional theory, generalized gradient approximation, pseudo-potential, geometry optimization*

Cite This Article: Humaira Takia, Md. Afjalur Rahman, Rahman Moshiur, M.M. Rahaman, and Khokon Hossen, "The Substantive Characteristics of Layered PbX (X=S, Se, and Te) Compounds: An ab-inito Investigations." *International Journal of Physics*, vol. 10, no. 2 (2022): 102-110. doi: 10.12691/ijp-10-2-3.

1. Introduction

With the ever increasing energy demand, decreasing of non-renewable energy supply it has been renewed interest about alternate energy sources. If new enormous and environmental friendly resources are not identified, the globe will become energy desert. The scientists are concerned about renewable energy sources, like Sun, wind and water current that can produce electricity. But sustainable technology has not been yet developed to store energy from these sources. The sun is the greatest renewable energy sources that could help to reduce the dependency on non-renewable energy sources such as fossil fuel. Therefore, researchers across the world are searching for efficient materials for harvesting solar energy and converting it in usable form. In condensed matter physics, computational materials science is an emerging field. The recent development of computational technique allows one to study a complex systems and physical properties of a material even without the information of experimental data [1,2]. More than 50 years lead chalcogenides PbS, PbSe and PbTe have been extensively studied by experiments due to their potential inflictions as energy converters and electronic devices [3]. They have also tempted great theoretical interest aimed at understanding the physics of their electronic band gaps, phase transitions and Ferro electric like behavior at low temperatures. As narrow gap semiconducting IV-VI compounds, lead chalcogenides demonstrate outstanding optical and electrical transport properties. On the other hand, they exhibit low thermal conductivities at high temperatures, which is unusual for simple structured materials. These unique features in electron and heat transport have made them practical thermoelectric

materials for a long time [4]. The bulk lead chalcogenides PbX, (X = S, Se, Te) have the cubic NaCl structure (space group Fm3m) and the direct narrow-gaps make them important in FETs [5], thermoelectric devices [6,7,8] and solar-energy panels [9]. At normal temperature and pressure Lead sulfide (PbS) and Lead telluride (PbTe) are like rock salt structure with direct band gap of about 0.45 eV and 0.29 eV respectively [10,11]. Lead selenide (PbSe) has also a stable rock-salt structure with direct band gap of 0.16 eV at 4 K [12]. The experiments as well as first principle calculations confirm direct band gap nature of these materials crystallize in NaCl-type structure at lower pressure, where adopt orthorhombic structure in the pressure range 2.5–6 GPa, however on further increase in pressure (13–25 GPa) they transform to CsCl type structure, metallic and superconductors [13] Many studies together with theoretical and experimental have been performed on the lead chalcogenides compounds. Ascertaining the worth of these materials, we have taken a step to study theoretically with these compounds and we believe that our study will be beneficial for further theoretical and experimental investigation on these compounds in the future.

In this study, ab initio calculations of the ground state has been conducted and different properties such as structural, elastic, electronic and optical properties of few-layer PbXs are explored theoretically by using the plane-wave pseudo-potential method within the generalized gradient approximation of the density functional scheme. The objective of the study is to carry out a complete DFT-based calculation to investigate the structural, elastic, electronic and optical properties (absorption, conductivity, reflectivity, refractive index, energy-loss spectrum, and dielectric function) of PbXs . Also stabilities of the few-layers are verified by the phonon bands and formation energies. In applications in Nano-electronics and opto-electronics, the tunable band gap and high carrier mobility indicate the high performance of few-layer PbX (X = S, Se, Te). The calculated adsorption of light indicates the potential applications of few-layer PbXs in solar cell. The residual part of this paper is organized as: Section II includes the computational method; Section III represents the results and discussion; and Section IV summarizes the concluding remarks.

2. Computational Methods

Based on the density functional theory, the First-principles calculations were carried out using the plane-wave pseudo-potential method [14] and implemented in the CASTEP code [15]. The electronic exchange-correlation energy is performed under the generalized gradient approximation (GGA) with the scheme of Perdew–Burke–Ernzerhof (PBE) [16]. The pseudo atomic calculations were performed for Pb- $5d^{10}6s^{2}6p^{2}$, S- $3s^{2}3p^{4}$, Se- $4s^{2}4p^{4}$, and Te-$5s^{2}5p^{4}$ as valence electrons respectively. In this calculation, the ultrasoft pseudo-potentials were used in a plane wave basis set with an energy cut-off of 350 eV and Monkhorst-Pack grid [17] of 8×8×8 k-points have been chosen for these materials. The symmetry of crystal structure is obtained via geometry optimization in the Broyden-Fletcher-Goldfarb-Shanno (BFGS) minimization scheme. Geometry optimization was performed using with the total energy of 1.0×10^{-5} eV/atom, the maximum force of 0.002 eV/Å, the maximum stress of 0.05 GPa and the maximum atomic displacement of 1×10^{-3} Å. These parameters were cautiously tested and adequate to carry a well converged total energy.

3. Results and Discussion

3.1. Structural and Elastic Properties

The lead chalcogenides (PbX) compounds has a NaCl-type structure of cubic lattice with a space group Fm-3m (225) [18]. In this calculation, lattice parameter has a value of 6.055Å, 6.259Å and 6.619Å for PbS, PbSe and PbTe respectively and the fractional coordinates in the unit cell of these compounds are 4a (0, 0, 0) for Pb and 4b (0.5, 0.5, 0.5) for S, Se and Te [13]. The atomic positions and lattice parameters have been optimized by minimizing the total energy as a function of normal stress. The optimized structure is shown in Figure 1. The optimized lattice parameter and unit cell volume at zero pressure for PbX (X=S, Se and Te) are listed in Table 1 including available experimental and other theoretical values. In the present study, the optimized lattice constants for PbS, PbSe, and PbTe are 5.930Å, 6.104 Å and 6.470 Å respectively. It is conspicuous from Table 1 that our predicted lattice parameters have a slightly contemptible deviation with the available experimental values. Elastic constants (C_{ij}) are calculated for the mechanical properties and dynamic information about the nature of the forces functioning in solids, which subsequently make relation to different basic solid-state phenomena like stability, ductility, brittleness, stiffness, and anisotropy [19]. Due to the cubic structures of PbX, individually it has three independent elastic constants C_{11}, C_{12}, and C_{44} at ambient pressure which are enlisted in Table 2.

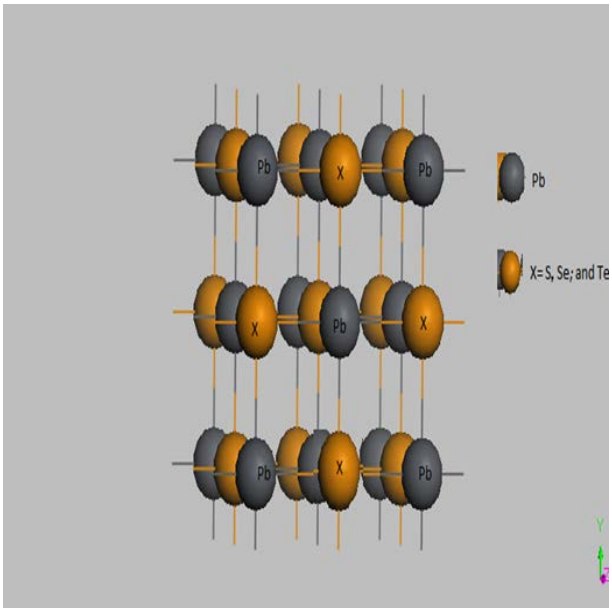

Figure 1. The crystal structures of lead chalcogenides, PbX (X=S, Se and Te): the conventional cubic cell

Table 1. The calculated equilibrium Lattice constants "a_0", unit cell volume "V_0" of PbS, PbSe and PbTe

Compounds	Properties	Expt. value	Other Calculation	Present Calculation	Deviation of a_0 from Expt.
PbS	a_0 (Å)	6.055Å [28] 5.9362 [29]	5.922 Å [30]	5.930	2.06%
	V_0 (Å^3)	221.99 [28]	-	208.34	
PbSe	a_0 (Å)	6.259Å [28] 6.1243 [29]	6.125 Å [30]	6.104	2.14%
	V_0 (Å^3)	245.19 [28]	-	227.45	
PbTe	a_0 (Å)	6.619Å [28] 6.4603 [29]	6.464 Å [30]	6.470	2.25%
	V_0 (Å^3)	289.98 [28]	-	271.31	

The independent elastic constants should fulfill the well-established Born stability conditions to belong to stable crystals mechanically. For cubic structures, the Born stability criteria are $C_{11} > 0$, $C_{44} > 0$; $C_{11} - C_{12} > 0$ and $C_{11} + 2C_{12} > 0$.

Table 2. The elastic constants *Cij* (GPa) and Cauchy pressure of PbS, PbSe and PbTe under ambient pressure

Compounds	C_{11}	C_{12}	C_{44}	C_{12}- C_{44}	
PbS	111.79	16.41	20.29	-3.88	This work
	135.1	16.9	20.4	-	[13]
PbSe	93.77	8.41	17.29	-8.88	This work
	123.6	12.2	17.6	-	[13]
	115.31	12.21	17.33	-	[20]
PbTe	92.70	3.26	14.85	-11.59	This work
	111	6.7	14.4	-	[13]

From Table 2, it is found that our investigated elastic constants are positive for all compounds and also fulfilling the above stability criteria. Thus, it can be concluded that all the compounds under study are mechanically stable in nature. The Cauchy pressure which is defined as $C_{12} - C_{44}$ could be used to explain the angular behavior of atomic bonding in metals and compounds [21]. If the value of Cauchy pressure is negative, the compound is expected to become non-metallic with directional bonding, while its positive value shows the metallic nature of materials [22]. Moreover, if it is negative, the material is expected to be brittle, but its positive value indicates the ductile manner of a material [21]. According to Table 2, it is clear that the calculated values of Cauchy pressure at an ambient condition are negative ensuring nonmetallic characteristics and brittleness manners of all the three compounds under study.

According to the calculated value of C_{ij}, the Voigt-Reuss-Hill (VRH) averaging scheme helps to determine the most significant solid-state phenomena of these compounds such as the bulk modulus B, shear modulus G, Young modulus Y, and Poisson's ratio ν [40]. The Voigt and Reuss limits of B and G for cubic crystal system can be expressed as follows [41]:

$$B_V = B_R = \frac{(C_{11} + 2C_{12})}{3} \quad (1)$$

$$G_V = \frac{(C_{11} - C_{12} + 3C_{44})}{5} \quad (2)$$

$$G_R = \frac{5C_{44}(C_{11} - C_{12})}{[4C_{44} + 3C_{11} - C_{12}]} \quad (3)$$

$$B = \frac{1}{2}(B_R + B_V) \quad (4)$$

$$G = \frac{1}{2}(G_R + G_V) \quad (5)$$

By using the following equations, Young's modulus (Y), and Poisson's ratio (ν) can be calculated.

$$Y = \frac{9GB}{3B + G} \quad (6)$$

$$\nu = \frac{3B - 2G}{2(3B + G)} \quad (7)$$

The calculated bulk modulus B, shear modulus G, Young modulus Y, Poisson's ratio ν, and B/G values for PbX have been tabulated in Table 3. From Table 3, it is seen that the value of bulk modulus B is greater than shear modulus G for all compounds indicating the shear modulus is the major parameter associated with the stability of cubic materials PbS, PbSe and PbTe [24]. B/G is defined as Pugh's ratio which could be used to make clear the ductility and brittleness behavior of a material. If the value of B/G is less than 1.75 for a material, it shows brittle nature or else is ductile. From Table 3, it is apparent that our calculated B/G ratio for all these compounds is less than 1.75 specifying that these materials behave in a brittle manner at ambient pressure. The similar result was obtained by investigating Cauchy's pressure which makes sure the consistency of our present study. The calculated value of Y for all the three phases reveals that the rigidity of these materials slightly increase according to the sequence PbTe <PbSe< PbS. The Poisson's ratio ν is used to reveal the stability of the compound against shear and gives information about the character of the bonding forces [25]. Its value is small (ν = 0.1) for covalent materials and for ionic materials the value is 0.25. The value ranges from 0.25 to 0.5 signifies that the force exists in the solid is central [26]. From our calculation, it is obvious that the value of ν for PbS, PbSe, and PbTe is very close to the value 0.25 indicating the dominant of the ionic nature of these compounds. For a completely isotropic compound, the value of the Zener anisotropy factors A is 1, whereas a value either smaller or larger than unity indicates the degree of elastic anisotropy. The value of A of PbX (X=S, Te, Se) is calculated by using the following formula and the calculated values have been listed in Table 3.

$$A = \frac{2C_{44}}{C_{11} - C_{12}} \quad (8)$$

Table 3. The bulk modulus *B* (GPa), shear modulus *G* (GPa), Young's modulus *Y* (GPa), *B/G* values, Poisson's ratio *ν* and anisotropy factor *A* of PbS, PbSe and PbTe at ambient pressure

Compounds	*B*	*G*	*Y*	*B/G*	*ν*	*A*	
PbS	48.20	27.72	69.78	1.74	0.26	0.43	This work
PbSe	36.86	24.51	60.19	1.50	0.23	0.41	This work
	53.97	764.82	304.21	-	0.26	-	[20]
PbTe	33.01	23.33	56.65	1.41	0.21	0.33	This work

It is observed from the calculated anisotropy values of PbX are less than unity. Hence, it can be concluded that all these materials under investigation exhibit a high elastic anisotropy.

3.2. Electronic Properties

Electronic properties can be obtained from the electronic band structure, total density of state (TDOS) and partial density of state (PDOS) along with the high symmetry direction of the Brillouin zone. Figure 2(a), Figure 2(b), and Figure 2(c) show the band structure of PbS, PbSe and PbTe respectively. The dotted line indicates the Fermi level between the conduction band and valence band along with the range of total band structure -15eV to 20eV. There is no energy level found that goes across Fermi level to overlap with the energy level of conduction band. At the *L* point of the Brillouin zone, the valence band is found maximum and the conduction band is found minimum for all three compounds. From the analysis of band structure diagram, it is obvious that all these compounds have semiconducting phase with a direct narrow band gap. The values of these band gaps are compared with literature data in the table below.

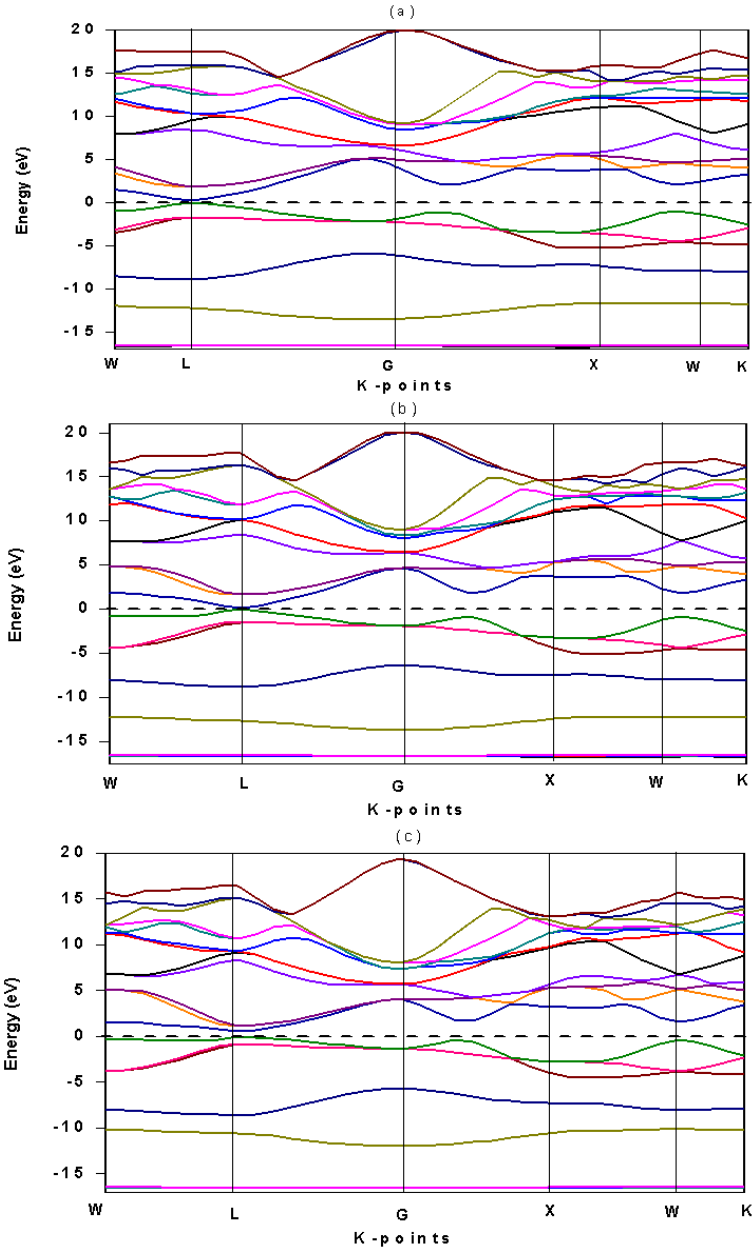

Figure 2. The electronic band structure of (a) PbS, (b) PbSe, and (c) PbTe Crystals along with high symmetry direction in the Brillouin zones

Table 4.

Compounds	PbS	PbSe	PbTe	
Band gap (eV)	0.23	0.15	0.58	This work
	[a]0.29, [b]0.41	[a]0.17, [c]0.29, 0.27[d]	[a]0.19	Experiment
	[e]0.25, [f]0.28	[e]0.30, [f]0.48	[e]0.41, [f]0.80	Theoretical

[a] [27], [b][28], [c] [20],[d] [29], [e] [30], and [f][31].

From Figure 3, it is observed that the lower part of valence band energy ranges from -17 eV to -11eV is composed of mainly from a strong hybridization of Pb-5d and S-3s states for PbS, Pb-5d and Se-4s for PbSe, and Pb-5d and Te-5s for PbTe respectively. At this part of valence band, for all phases, Pb-5d plays central role. The middle part of valence band, which is found at -8.5 eV to -5.5 eV, is made up from mainly Pb-6s state for these materials with slightly admixture of S-3p and S-3s states in case of PbS, Se-4s and Se-4p states for PbSe, and Te-5s and Te-5p states for PbTe. The next part is the upper part of valence band (-5.5 eV to below Fermi level) which is near to the Fermi level. The prevalent contribution comes from S-3*p* states for PbS, Se-4*p* in case of PbSe, and Te-5*p* in case of PbTe with a little contribution of Pd-6*p* and Pb-6*s* individually for all compounds. This part is mainly propagates from Pb-5d and S-3p states in case of PbS, Pb-6p and Se-4p states in case of PbSe, Pb-6p and Te-5p states in case of PbTe whereas the contribution of Pb-6p states is supreme for PbSe and PbTe compounds.

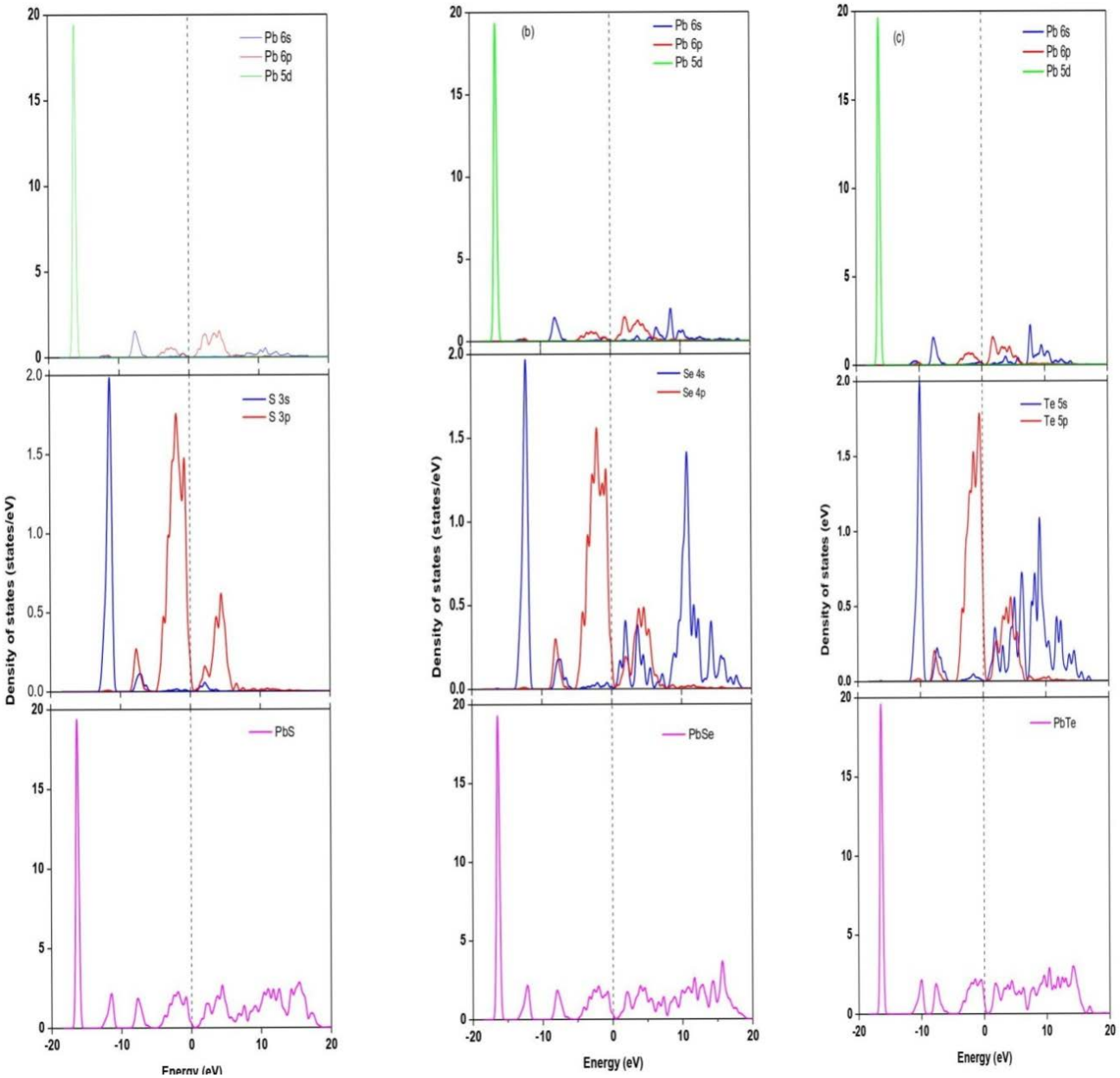

Figure 3. Total and partial density of states for (a) PbS, (b) PbSe and (c) PbTe

The conduction band mainly contributes form S-3p and Pb-5d states in case of PbS, Se-4p and Pb-6p states in case of PbSe and Te-5p and Pb-6p states in case of PbTe whereas Pb-6p orbital is dominant. Now, above the Fermi level, the lower part of conduction band is composed of Pb-6*p* and S-3*p* states for PbS, whereas the upper part of conduction band is dominated by Pb-6s, Pb-6p with a slight contribution of S-3p state. For PbSe, the lower part of conduction band is dominated by Pb-6*p* with S-3*p*and S-3p states, while in the upper part, Se-4s plays vital role. In case of PbTe, the lower part and upper part of conduction band is composed of small admixture of Pb-6s, Pb-6p, Te-5s, andTe-5p states.

3.3. Optical Properties

The optical functions of solids provide a perception of the electronic configuration of compounds. Different optical parameters for PbX at different photon energies have been demonstrated using frequency dependent dielectric function which is defined as $\varepsilon(\omega) = \varepsilon_1(\omega) + i\varepsilon_2(\omega)$ and it is closely associated with the electronic band structure. The imaginary part $\varepsilon_2(\omega)$ of the complex dielectric function is found from the momentum matrix elements between the occupied and the unoccupied electronic states and calculated directly using equation (9)

$$\varepsilon_2(\omega) = \frac{2e^2\pi}{\Omega\varepsilon_0} \sum_{k,v,c} \left| \left\langle \psi_k^c \left| \hat{u} \cdot \vec{r} \right| \psi_k^v \right\rangle \right|^2 \delta(E_k^c - E_k^v - E) \quad (9)$$

where ω is the frequency of light, e is the electronic charge, Ω is the unit cell volume, $\hat{u}$ is the vector defining the polarization of the incident electric field, ψ_k^c and ψ_k^v are the conduction and valence band wave functions at k respectively. The real part of the dielectric function $\varepsilon_1(\omega)$ is derived from the imaginary part of the dielectric function $\varepsilon_2(\omega)$ using the Kramers-Kronig relations. On the other hand, other optical properties such as refractive index, absorption spectrum, reflectivity and conductivity (real part) are derived from the following equations.

$$N = n + ik \quad (10)$$

$$\eta = \frac{2k\omega}{c} \quad (11)$$

$$R = \left| \frac{1-N}{1+N} \right|^2 = \frac{(n-1)^2 + k^2}{(n+1)^2 + k^2} \quad (12)$$

$$\sigma = \sigma_{1+} i\sigma_2 = -i\frac{\omega}{4\pi}(\varepsilon - 1) \quad (13)$$

Moreover, the energy loss function of a material, which can be calculated from the complex dielectric constant, describes the energy lost when an electron passes through a homogeneous dielectric material and is given by [32].

$$I_m\left(\frac{-1}{\epsilon(\omega)}\right) \quad (14)$$

Figure 4 demonstrates the optical functions of PbX (where X = S, Se and Te) calculated for photon energies up to 40 eV for polarization vector [100]. We have used a 0.5 eV Gaussian smearing for all calculations because this smears out the Fermi level.

The absorption coefficient data give information about solar energy conversion efficiency and how far light of specific frequency can impinge into a material before being absorbed [32]. Figure 4 depicts the absorption coefficient of PbX (where X=S, Se and Te). It is obvious that the absorption of these phases starts at slightly above 0 eV (around 0.01ev) which represents the semi-metallic characteristics of PbX (where X=S, Se and Te). From Figure-4 (a), It has been seen that the nature of absorption curves are almost same from 0.1 – 30 eV for all these compounds. At various energy ranges, several absorption peaks are observed also. The prominent absorption peak is found at energy approximate ranges from 30 to 35 eV for all these compounds.

At this energy range, the value of the absorption peaks of PbS and PbSe are almost double comparing with PbTe. In addition, all the compounds show rather good absorption coefficient in the low energy region at about 0.1 – 15eV and also in the high energy region at around 30-35 eV.

The investigated conductivity spectra with photon energy upto 40 eV of PbX (X = S, Se and Te) are shown in Figure 4 (b). From this figure, it is observed that photoconductivity starts slightly above zero photon energy due to the reason that the materials have a narrow band gap which is also evident from the band structure indicating the semi-metallic behaviors of these phases. It is also seen that all these materials are highly conductive in the low energy region (0.1-5 eV). All the compounds belong to several maxima and minima peaks within the energy ranges about 5-35 eV and no photoconductivity is found above 35 eV.

The reflectivity spectra of PbX (X = S, Se and Te) as a function of photon energy are illustrated in Fig.4(c). It is noticed that reflectivity is high in the infrared region for all these phases and among them PbSe exhibits slightly greater reflectivity comparing with the others. The reflectivity peaks can also be observed in the energy ranges (30-35 eV) for these three materials, where PbS shows the prominent reflectivity peak than the other materials in this high energy region. The higher reflectivity spectra of these compounds in the Infrared and ultraviolet regions show promise as excellent coating materials for avoiding solar heating. The energy loss functions of a material as a function of photon energy is an important optical parameter that describes the loss of energy of a prompt electron passing through that material and becomes larger at the plasma frequency [33]. It is defined by the bulk plasma frequency ω_p which occurs at $\varepsilon_2 < 1$ and $\varepsilon_1 = 0$ [34]. The energy loss functions for all these three compounds under investigation are depicted in Figure 4(d). In the energy-loss spectrum, we see that all compounds correspond to the similar plasma frequency ω_p with the approximated value about 35 eV specifying that these material PbX (X = S, Se and Te) will be transparent when the incident photon energies are greater than 35 eV. In addition, the peaks found from loss function correspond to the trailing ends in reflection spectra.

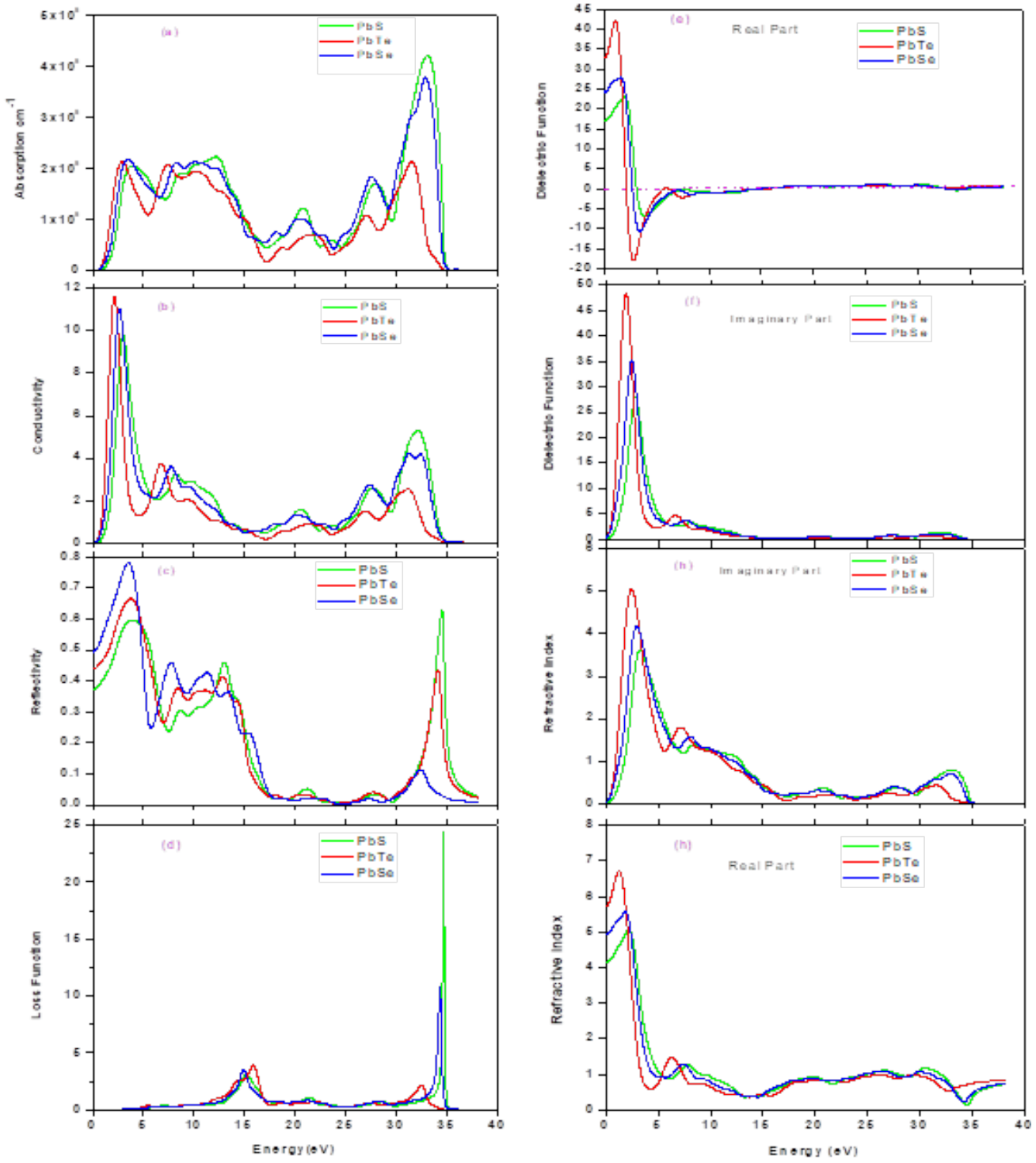

Figure 4. The calculated optical functions of PbX (where X=S, Se and Te): (a) absorption, (b) conductivity, (c) reflectivity, (d) loss function, (e) real part of dielectric function, (f) imaginary part of dielectric function, (g) imaginary part of refractive index and (h) real part of refractive index in the polarization vector [100]

The Dielectric function explains the most general property of solids of a material such as polarization and absorption properties when electromagnetic wave passes through it. The real and imaginary parts of dielectric constants have been plotted as a function of photon energy as shown in Figure 4(e) and Figure 4(f). It is obvious from the study that for all phases $\varepsilon_2(\omega)$ become zero at about 35 eV indicating that all materials becomes transparent at above 35 eV. Generally, the nonzero value of $\varepsilon_2(\omega)$ indicates the starting of absorption of photon energy by the material. Thus, it is clear that the observation found from dielectric function corroborates the observation found from the absorption spectra diagram Figure 4(a) that indicates the reliability of our work. The static dielectric constants of PbS, PbSe, and PbTe are around 17, 25 and 34 respectively, which indicate the compounds as dielectric material. The refractive indices in terms of imaginary and real parts of PbX (X = S, Se and Te) are displayed in Figure 4(g) and Figure 4(h). The imaginary part explains the amount of absorption loss of

electromagnetic wave while passes throughout the material and the real part signifies the phase velocity. From Figure 4 (h), it is observed that the static refractive indices start with a higher value of ~4.1, 4.9 and 5.8 respectively for PbS, PbSe, and PbTe in the infrared region due to the inter band transition, and all these values drop in the high energy region with some several peaks.

4. Conclusions

In epitome, we have systemically explored the structural, elastic, electronic and optical properties of the halite cubic narrow-gap semiconductors PbX (X=S, Se and Te) based on density functional theory which are performing the generalized gradient approximation (GGA). Here our calculated lattice parameters for all compounds have a minute variation from available experimental data and other theoretical findings. We have also evaluated the independent elastic constants, Young's modulus, bulk modulus, shear modulus, Poisson's ratio, compressibility and elastic anisotropy factor. The materials show elastically anisotropic and brittle nature. They are also found to be mechanically stable conditions. The investigated band structure, Density of states, and optical properties ensure the semi-metallic behavior of PbX (X= S, Se, Te) with a narrow gap of 0.23 eV, 0.15 eV, and 0.58 eV for PbS, PbSe, and PbTe respectively. The optical properties such as absorption spectra, conductivity, reflectivity, loss function, dielectric function and refractive index have been determined and analyzed in details. From the study of the optical function in [100] direction, it is observed the reflectivity is larger in the infrared and ultraviolet regions which indicates that all these compounds would be used as possible shielding material as like the solar cell to remove solar heating as a coating for ultraviolet radiation. For future investigations, the present study has an eminent adhesion on the physical and superconducting properties of other rock-salt superconductors. We anticipate that our present study on this narrow-gap semiconductor would facilitate to headway in this field.

Acknowledgements

The authors gratefully acknowledge the tremendous support provided by Dept. of Physics, PUST; Dept. of PME & Mathematics, PSTU; Dept. of Physics, JU as well as Bangladesh Atomic Energy Commission.

References

[1] Mun Wong, K., Alay-e-Abbas, S. M., Shaukat, A., Fang, Y., & Lei, Y., "First-principles investigation of the size-dependent structural stability and electronic properties of O-vacancies at the ZnO polar and non-polar surfaces," Journal of Applied Physics, 113(1), 014304.2013.

[2] Mun Wong, K., Alay-e-Abbas, S. M., Fang, Y., Shaukat, A., & Lei, Y., "Spatial distribution of neutral oxygen vacancies on ZnO nanowire surfaces: an investigation combining confocal microscopy and first principles calculations," Journal of Applied Physics, 114(3), 034901.2013.

[3] Dalven, R., "Electronic Structure of PbS, PbSe, and PbTe," In Solid State Physics (Vol. 28, pp. 179-224). Academic Press.1974.

[4] L. K. Y. R. T. S. BA Efimova, "Thermoelectric Figure of Merit of N-Type PbTe," Sov. Phys. Semicond, vol. 4, p. 1653, 1971.

[5] Oh, S. J., Berry, N. E., Choi, J. H., Gaulding, E. A., Paik, T., Hong, S. H., ... & Kagan, C. R., "Stoichiometric control of lead chalcogenide nanocrystal solids to enhance their electronic and optoelectronic device performance," ACS nano, 7(3), 2413-2421. 2013.

[6] Biswas, K., He, J., Blum, I. D., Wu, C. I., Hogan, T. P., Seidman, D. N., ... & Kanatzidis, M. G., "High-performance bulk thermoelectrics with all-scale hierarchical architectures," Nature, 489(7416), 414-418.2012.

[7] Heremans, J. P., Jovovic, V., Toberer, E. S., Saramat, A., Kurosaki, K., Charoenphakdee, A., ... & Snyder, G. J., "Enhancement of thermoelectric efficiency in PbTe by distortion of the electronic density of states ," Science, 321(5888), 554-557.2008.

[8] Girard, S. N., He, J., Zhou, X., Shoemaker, D., Jaworski, C. M., Uher, C., ... & Kanatzidis, M. G., "High performance Na-doped PbTe–PbS thermoelectric materials: electronic density of states modification and shape-controlled nanostructures," Journal of the American Chemical Society, 133(41), 16588-16597.2011.

[9] Aerts, M., Bielewicz, T., Klinke, C., Grozema, F. C., Houtepen, A. J., Schins, J. M., & Siebbeles, L. D., "Highly efficient carrier multiplication in PbS nanosheets," Nature communications, 5(1), 1-5. 2014.

[10] Qadri, S. B., Singh, A., & Yousuf, M., "Structural stability of PbS films as a function of temperature," Thin Solid Films, 431, 506-510. 2003.

[11] Leitsmann, R., Bechstedt, F., Groiss, H., Schäffler, F., Heiss, W., Koike, K., ... & Yano, M., "Structural and electronic properties of PbTe (rocksalt)/CdTe (zinc-blende) interfaces," Applied surface science, 254(1), 397-400.2007.

[12] Paul, A., & Klimeck, G.,"Atomistic study of electronic structure of PbSe nanowires," Applied Physics Letters, 98(21), 212105. 2011.

[13] Zhang, Y., Ke, X., Chen, C., Yang, J., & Kent, P. R. C., "Thermodynamic properties of PbTe, PbSe, and PbS: First-principles study," Physical review B, 80(2), 024304.2009.

[14] Kohn, W., & Sham, L. J., "Self-consistent equations including exchange and correlation effects," Physical review, 140(4A), A1133.1965.

[15] Clark, S. J., Segall, M. D., Pickard, C. J., Hasnip, P. J., Probert, M. I., Refson, K., & Payne, M. C., "First principles methods using CASTEP," Zeitschrift für kristallographie-crystalline materials, 220(5-6), 567-570. 2005.

[16] Perdew, J. P., Burke, K., & Ernzerhof, M., "Generalized gradient approximation made simple," Physical review letters, 77(18), 3865. 1996.

[17] Monkhorst, H. J., & Pack, J. D. (1976), "Special points for Brillouin-zone integrations," Physical review B, 13(12), 5188. 1976.

[18] Han, G., Zhang, R., Popuri, S. R., Greer, H. F., Reece, M. J., Bos, J. W. G., ... & Gregory, D. H., "Large-scale surfactant-free synthesis of p-Type SnTe nanoparticles for thermoelectric applications," Materials, 10(3), 233. 2017.

[19] Edrees, S. J., Shukur, M. M., & Obeid, M. M., "First-principle analysis of the structural, mechanical, optical and electronic properties of wollastonite monoclinic polymorph," Computational Condensed Matter, 14, 20-26.2018.

[20] E. I. A. a. T. C. Chibueze, "Ab-initio study of structural, elastic, electronic and vibrational properties of PbSe in the rock-salt structure," Adamawa State University Journal of Scientific Research, vol. 7, no. 2, p. 205, 2019.

[21] Pettifor, D. G., "Theoretical predictions of structure and related properties of intermetallics," Materials science and technology, 8(4), 345-349.1992.

[22] W.-C. H. D.-j. L. X.-Q. Z. C.-S. X. X.-J. Y. Yong Liu, "First-principles investigation of structural and electronic properties of MgCu2 Laves phase under pressure," Intermetallics, vol. 31, p. 357, 2012.

[23] Z.-j. a. Z. E.-j. a. X. H.-p. a. H. X.-f. a. L. X.-j. a. M. J. Wu, "Crystal structures and elastic properties of superhard IrN_2 and IrN_3 from first principles," Phys. Rev. B, vol. 76, no. 5, p. 054115, 2007.

[24] Liu, Q. J., Liu, Z. T., Feng, L. P., & Tian, H., "First-principles study of structural, elastic, electronic and optical properties of rutile GeO_2 and α-quartz GeO_2," Solid state sciences, 12(10), 1748-1755.2010.

[25] J. Z. Y. L. Z. N. Z. L. Yong Cao, "First-principles studies of the structural, elastic, electronic and thermal properties of Ni3Si," Computational Materials Science, vol. 69, p. 40, 2013.

[26] Pfrommer, B. G., Côté, M., Louie, S. G., & Cohen, M. L., "Relaxation of crystals with the quasi-Newton method," Journal of Computational Physics, 131(1), 233-240.1997.

[27] Schmidt-Kaler, T., "Numerical data and functional relationships in science and technology," Landolt-Bornstein, 2, 15-18.1982.

[28] Ni, Y., Liu, H., Wang, F., Liang, Y., Hong, J., Ma, X., & Xu, Z., "PbS crystals with clover-like structure: Preparation, characterization, optical properties and influencing factors," Crystal Research and Technology: Journal of Experimental and Industrial Crystallography, 39(3), 200-206.2004.

[29] Streltsov, S. V., Manakov, A. Y., Vokhmyanin, A. P., Ovsyannikov, S. V., & Shchennikov, V. V., "Crystal lattice and band structure of the intermediate high-pressure phase of PbSe," Journal of Physics: Condensed Matter, 21(38), 385501. 2009.

[30] Khan, A. A., Khan, I., Ahmad, I., & Ali, Z., "Thermoelectric studies of IV-VI semiconductors for renewable energy resources," Materials Science in Semiconductor Processing, 48, 85-94. 2016.

[31] Z. A. S. J. K. Y. A. S. H. a. M. S. Asghar Khan M, "Principle Investigation of Structural, Electronics and Chemical Properties of Sn Doped PbX (X=S, Se, Te)," J Theor Comput Sci, vol. 4.2, 2017.

[32] R. Atikur and R. A. a. R. Zahidur, "First-Principles Calculations of Structural, Electronic and Optical Properties of $HfZn_2$," Journal of Advanced Physics, vol. Volume 5, no. 4, p. 354, 2016.

[33] Rahman, M. A., Rahaman, M. Z., & Rahman, M. A., "The structural, elastic, electronic and optical properties of MgCu under pressure: A first-principles study," International Journal of Modern Physics B, 30(27), 1650199. 2016.

[34] Y. L.-H. S. T. a. F. A. J. Saniz R,"Structural, electronic, and optical properties of $NiAl_3$: First-principles calculations," Physical Review B, vol. 74, no. 1, p. 014209, 2006.

[35] Zhang, Y., Ke, X., Chen, C., Yang, J., & Kent, P. R. C., "Thermodynamic properties of PbTe, PbSe, and PbS: First-principles study," Physical review B, 80(2), 024304. 2009.